Novel Phase Separation and Spin Dynamics of Lightly Doped $La_{2-x}Sr_2CuO_4$ Probed by La-Nuclear Quadrupole Resonance

K. Ishida,[1,*] H. Aya,[1] Y. Tokunaga,[1,†] H. Kotegawa,[1,‡] Y. Kitaoka,[1] M. Fujita,[2,§] and K. Yamada[2,§]

[1]*Department of Physical Science, Graduate School of Engineering Science, Osaka University, Toyonaka, 560-8531, Japan*

[2]*Institute for Chemical Research, Kyoto University, Uji 610-0011, Japan*

(Received 10 September 2003; published 22 June 2004)

We report novel magnetic properties in the slightly hole-doped Mott-insulator $La_{2-x}Sr_xCuO_4$ via the La-nuclear quadrupole resonance (NQR) measurements. At $x = 0.018$, the *antiferromagnetic* (AFM) La-NQR spectrum affected by internal fields comes out as the temperature decreases below $T_N \sim 150$ K, whereas the *nonmagnetic* one persists to be observed down to a temperature $T_f \sim 20$ K at which the nuclear-relaxation rate has a pronounced peak. This demonstrates that the phase separation of nonmagnetic and AFM phases occurs between T_f and T_N. The novel phase separation is suggested as due to the *partial destruction of the AFM phase* caused by mobile holes via the formation of an extended spin-singlet state between Cu-derived spins and hole spins.

DOI: 10.1103/PhysRevLett.92.257001 PACS numbers: 74.72.Dn, 74.25.Ha, 75.30.Kz, 76.60.Gv

Since the discovery of high-T_c cuprate superconductors, magnetic properties of *slightly hole-doped Mott insulators* have been extensively investigated from theoretical and experimental aspects to elucidate a physical background of cuprate superconductors [1]. In this context, $La_{2-x}Sr_xCuO_4$ (LSCO) is a most suitable system since the undoped La_2CuO_4 is a well-known three-dimensional (3D) antiferromagnetic (AFM) compound. The holes are doped into AFM CuO_2 planes by substituting divalent Sr^{+2} for trivalent La^{3+}. Until now, there have not been many reports about the magnetic properties in a slightly doped region where a 3D AFM order is suddenly suppressed by doping holes.

The slightly doped LSCO compounds for $x \leq 0.02$ were extensively investigated via the microscopic tools such as La-nuclear quadrupole resonance (NQR)/NMR, and muon spin rotation (μSR) by Borsa and co-workers [2–4]. The Cu-derived local AFM moment $M(x, T)$ below T_N revealed that $M(x, T)$ above 30 K is progressively depressed as T and x increase, but it is unexpected that $M(x, T)$ is markedly increased upon cooling below 30 K. $M(x, T)$ is nearly independent of x at a low temperature, being almost the same as the value for undoped La_2CuO_4. Such an increase in $M(x, T)$ was interpreted by the localization of doped holes below 30 K. As a result, it was suggested that mobile holes are much more effective in reducing $M(x, T)$ than localized holes.

On the other hand, different from these results, neutron-scattering (NS) experiments on lightly doped LSCO revealed that a diagonal spin modulation takes place in the spin-glass phase in $0.02 \leq x \leq 0.055$ [5–7]. Note that this is a one-dimensional modulation rotated away by 45° from the parallel modulation in the superconducting phase in $0.055 \leq x$. An ordered moment below 30 K is extrapolated to the value of $\sim 0.1\mu_B$ at $x = 0.02$ that is much smaller than $0.48\mu_B$ in the undoped La_2CuO_4 [8]. Furthermore, the elastic NS measurements revealed that a magnetic Bragg NS intensity develops below T_N but starts to be decreased below $\sim$30 K (T_f), probing an onset of a reentrant spin-glass order. It should be noted that the La-NQR/NMR and μSR deduced nearly the same values for T_N and T_f as the NS did, whereas former experiments deduced a $M(x, T)$ comparable to the value for La_2CuO_4 that is significantly larger than the NS did. This means that the sizes of the AFM moments below T_f are not consistent with each other.

In addition, transport properties in the slightly doped LSCO were studied by Ando *et al.* [9]. They demonstrated the metallic charge transport even in the heavily underdoped LSCO at moderate temperature and demonstrated that in-plane resistivity keeps its metallic behavior well below T_N. This clearly shows that the in-plane charge transport is insensitive to the long-range magnetic order.

To shed further light on the magnetic character in the lightly doped LSCO compounds and the relation between the magnetic and transport properties, in this Letter we report on a precise La-NQR study on lightly doped LSCO single crystals at $x = 0.01$, 0.018, and 0.024. By contrast to the previous reports by Borsa *et al.* [4], we here focus on the low NQR transition at $1\nu_Q(\pm 1/2 \leftrightarrow \pm 3/2)$. This is because the $1\nu_Q$ transition can sensitively probe internal fields $H_{\rm int}$ due to any type of static magnetic order. Both internal fields parallel ($H^c_{\rm int}$) and perpendicular ($H^{ab}_{\rm int}$) to the principal c axis split the $1\nu_Q$-NQR spectrum into two doublets, whereas each spectrum at the $2\nu_Q$ ($\pm 3/2 \leftrightarrow \pm 5/2$) and the $3\nu_Q$ ($\pm 5/2 \leftrightarrow \pm 7/2$) transition is split into one doublet by $H^c_{\rm int}$. The splitting in $1\nu_Q$-NQR due to the $H^{ab}_{\rm int}$ is about 4 times larger than that due to the $H^c_{\rm int}$, allowing us to distinguish the NQR spectrum associated with a magnetic phase from others if any. As a matter of fact, the $1\nu_Q$- La-NQR from the AFM phase at $x = 0.018$ is well separated from that from some nonmagnetics phases below T_N, providing clear evidence for the

magnetic phase separation. Furthermore, the nonmagnetic phase disappears below $T_f \sim 20$ K, at which the nuclear spin-lattice relaxation rate $1/T_1$ and the nuclear spin-spin relaxation rate $1/T_2$ show a maximum. It is demonstrated that the novel magnetic phase separation occurs in a T range between T_f and T_N at $x = 0.018$. We remark that this phase separation is associated with the presence of mobile holes, and hence their localization is responsible for making fluctuating spin degrees of freedom freeze below T_f. The present experiment reveals that extended nonmagnetic state is embedded in the AFM phase by slightly doping mobile holes.

In the present experiment, we used the same single crystals LSCO at $x = 0.01$, 0.018, and 0.024 as in NS and other measurements [8,10].

Figure 1 shows the temperature (T) dependence of the NQR spectra for the $1\nu_Q$ transition at (a) $x = 0.01$ and (b) $x = 0.018$. For $x = 0.01$, the two-doublet NQR spectra are observed below $T_N \sim 240$ K, associated with $H^c_{\rm int}$ and $H^{ab}_{\rm int}$. This change in spectrum below T_N resembles that in La_2CuO_4 [4]. It should be, however, noted that a weak but visible NQR spectrum originating from the paramagnetic phase remains even at 200 K below T_N but disappears at 170 K. On the other hand, at $x = 0.018$, it is surprising that nonmagnetic NQR spectrum remains dominant down to 15 K far below $T_N \sim 150$ K estimated from other measurements [10]. By contrast, the weak but visible magnetic one is also apparent below T_N. This gives clear microscopic evidence for the magnetic phase separation below T_N.

Figure 2 shows the T dependence of $H^{ab}_{\rm int}$ derived from the separation between the two doublets in the La-NQR below T_N (see Fig. 1). The $H^{ab}_{\rm int}$ at $x = 0.01$ increases rapidly below T_N, followed by a slight increase below 30 K, whereas the $H^{ab}_{\rm int}$ at $x = 0.018$ increases *gradually* below T_N with a pronounced increase below 20 K. Note that an unchanged ratio $H^c_{\rm int}/H^{ab}_{\rm int} \sim 0.2$ down to low T indicates no change in the direction of the ordered moment. Therefore, the increase in $H^{ab}_{\rm int}$ below 20 K is not ascribed to the change in the direction of AFM moments but to the increase of their size. We remark that the $H^{ab}_{\rm int}$ at $x = 0.018$ in 20 K $< T < T_N$, which is much smaller than that at $x = 0.01$, develops rather gradually upon cooling below T_N, and that $H^{ab}_{\rm int}$ reaches the same value at the lowest T. The former is due to the increase in density of holes, whereas the latter is ascribed to the localization of holes at low T. The magnetic phase separation at $x = 0.018$, which is characterized by a large fraction of nonmagnetic phase down to low T far below T_N, should be relevant with the presence of holes, even though its doping level seems to be not large enough.

Figure 3 shows the T dependence of the La-NQR intensity $I(T)$ for the nonmagnetic fraction multiplied by T, $[I(T) \times T]$. The NQR intensity depends on T_2 with the relation of $I(\tau) = I(\tau = 0)\exp(-2\tau/T_2)$ where τ is a pulse interval between two pulses for the spin-echo measurement. When $I(\tau = 0) \times T$ is normalized by the value at $T_N = 150$ K, it is expected that $I \times T$ would be nearly constant in the paramagnetic state if nothing happens. However, it gradually decreases upon cooling below T_N as seen in the figure. This shows that the La-NQR spectrum for the nonmagnetic phase is partially wiped out due to the emergence of the AFM phase upon cooling below T_N. The nonmagnetic NQR spectral intensity becomes weaker with decreasing T, as shown in Fig. 3, and disappears around $T_f \sim 20$ K. Note that the full width at half maximum (FWHM) for the nonmagnetic NQR spectrum is almost independent down to $T = 50$ K and increases gradually below 50 K due to the increase of $1/T_2$ as shown in the inset. This proves that most of region in the nonmagnetic phase is not coupled with the AFM phase, even though the former phase is embedded in the latter phase. A ratio of AFM to nonmagnetic phase becomes T dependent between T_f and T_N, which gives clear

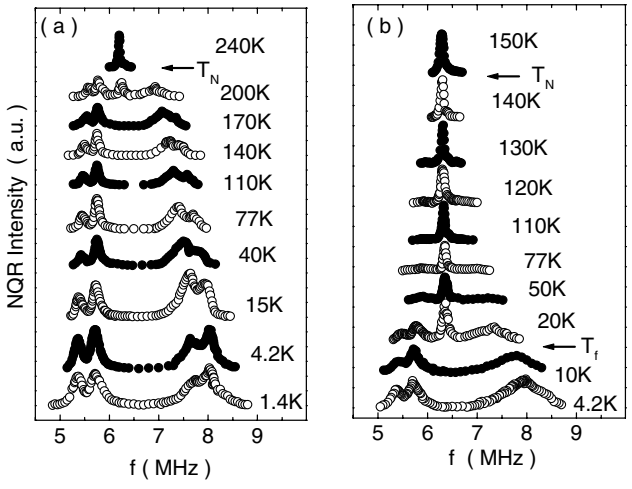

FIG. 1. La-NQR spectra of the $\nu_Q(\pm 1/2 \leftrightarrow \pm 3/2)$ transition in (a) $x = 0.01$ and (b) $x = 0.018$, respectively.

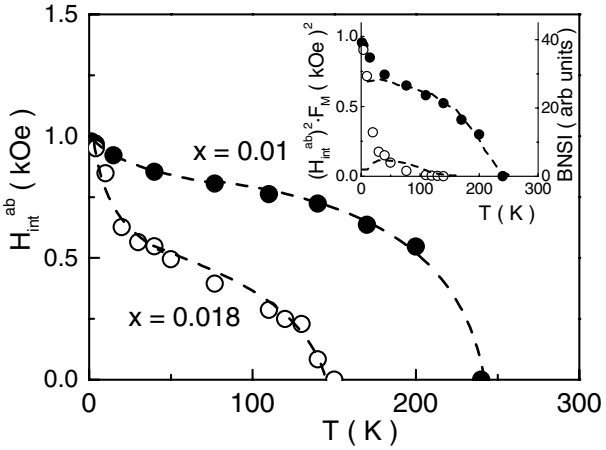

FIG. 2. Internal fields perpendicular to the c axis, $H^{ab}_{\rm int}$ of the magnetic site. The inset shows $(H^{ab}_{\rm int})^2$ multiplied by a magnetic volume fraction F_m, which is a comparable value of the Bragg neutron-scattering intensity (BNSI). T dependence of the BNSI is shown by dotted lines (see in text).

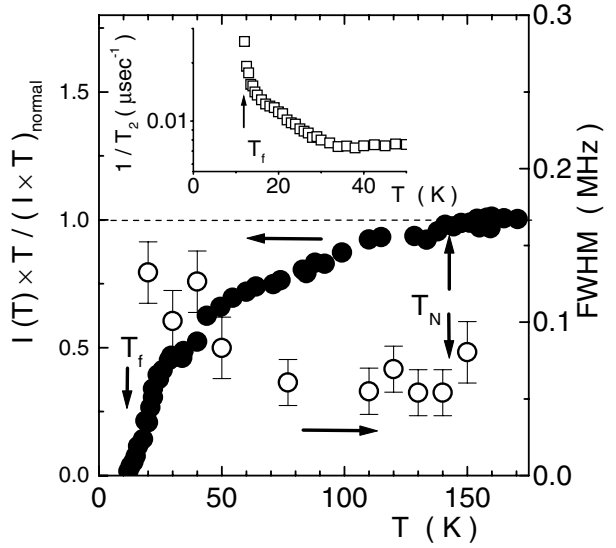

FIG. 3. T-normalized NQR signal intensity $I(T)T$ from the non-magnetic site divided by the IT at 150 K (normal state) is plotted against T. The FWHM of the non-magnetic signal is also shown. The inset shows the temperatue dependence of $1/T_2$ at the non-magnetic site.

evidence for the magnetic phase separation below T_N at $x = 0.018$. The remarkable result is that the true long-range AFM order collapses already at such a low doping level as $x = 0.018$ where AFM order had been believed to be established from the various measurements. Instead, the magnetic phase separation takes place below $T_N = 150$ K, and the magnetically ordered state over the whole sample is realized below $T_f \sim 20$ K. At $x = 0.024$, the AFM La-NQR spectrum is not observed at all down to very low T comparable to T_f for $x = 0.018$ without any evidence for the magnetic phase separation.

To gain further insight into an origin for the novel phase separation, we compare our results with those obtained by the NS experiments [8]. The Bragg neutron-scattering intensity (BNSI) is proportional to a square of $M_B(x, T)$ and the volume fraction of the magnetic phase, F_m. Using the NQR intensity $I(T)$ for the volume fraction of the nonmagnetic phase, $F_m \sim 1 - I(T)T/IT_{\text{normal}}$ is estimated. Here, IT_{normal} is a constant value in a T range above $T = 150$ K. The BNSI is related to the value of $(H_{\text{int}}^{ab})^2 F_m$ since $(H_{\text{int}}^{ab}) \sim M_B(x, T)$. The inset of Fig. 2 indicates $(H_{\text{int}}^{ab})^2 F_m$ vs T plot together with the T dependence of BNSI shown by the dotted curve. As seen in the figure, $(H_{\text{int}}^{ab})^2 F_m$ is enhanced below 50 K in $x = 0.01$ and 0.018. By contrast, the BNSI at a commensurate wave vector $\mathbf{Q}_c = (1, 0, 0)$ starts to decrease upon cooling below $T_f \sim 30$ K, whereas it is remarkable that the additional magnetic NS intensity $M_{\text{IC}}(x, T)$ develops at the diagonal incommensurate (IC) wave vector $\mathbf{Q}_c = (0, 1 - \delta, 0)$. It should be noted that the increase in H_{int}^{ab} below $T_f \sim 30$ K is closely relevant with the growth of $M_{\text{IC}}(x, T)$. By contrast, $(H_{\text{int}}^{ab})^2 F_m$ at the low T stays a constant regardless of x, whereas $M_B(x, T)^2 + M_{\text{IC}}(x, T)^2$ decreases with increasing x. This is related to the fact that the La-NQR results probing the local magnetic state differ from the NS results probing the spatially correlated magnetic state as suggested by Matsuda *et al.* [8].

Now we note the novel magnetic properties in the nonmagnetic fraction in the phase separated state. Figure 4 shows the T dependence of $1/T_1$ at the nonmagnetic and AFM sites at $x = 0.018$, together with $1/T_1$ for $x = 0.01$ that was measured at the $3\nu_Q$ transition ($f = 19$ MHz). The $1/T_1$ at $x = 0.01$ starts to decrease below $T \sim 220$ K, which is slightly lower than $T_N \sim 240$ K, and is enhanced remarkably below 50 K. $1/T_1$ shows a clear maximum at $T_f \sim 20$ K, at which some spin freezing is suggested by NQR and μSR measurements [2,4,11]. The behavior of $1/T_1$ in $x = 0.01$ is in good agreement with the previous result by Chou *et al.* [2]. By contrast for $x = 0.018$, the $1/T_1$ at the nonmagnetic site does not show any anomaly at T_N and continues to increase down to T_f, whereas $1/T_1$ at the AFM site seems to show a slight decrease below T_N as in $x = 0.01$. The T dependence of $1/T_1$ in the phase separated state below T_N is different at the nonmagnetic and AFM sites. The critical magnetic fluctuations towards T_N are not present at all at the nonmagnetic site. This nonmagnetic region may be extended by mobile holes to form the spin-singlet state between Cu spins and hole spins. In this context, spin dynamics are governed by possible dynamics of holes, but not by Cu-spin dynamics.

In general, when the correlation function of local-field fluctuations is assumed to be of an exponential type as $\langle h(0)_+, h(t)_- \rangle \sim \langle h \rangle^2 \exp(-2t/\tau_c)$, where τ_c is the correlation time, $1/T_1$ is expressed as

$$\left(\frac{1}{T_1}\right) \sim \frac{\gamma^2}{2} \int \overline{\langle h(0), h(t) \rangle} e^{-i\omega_n t} dt \sim (\gamma_n \overline{h})^2 \frac{\tau_c}{1 + (\omega_n \tau_c)^2},$$

where ω_n is an NQR frequency. It was pointed out

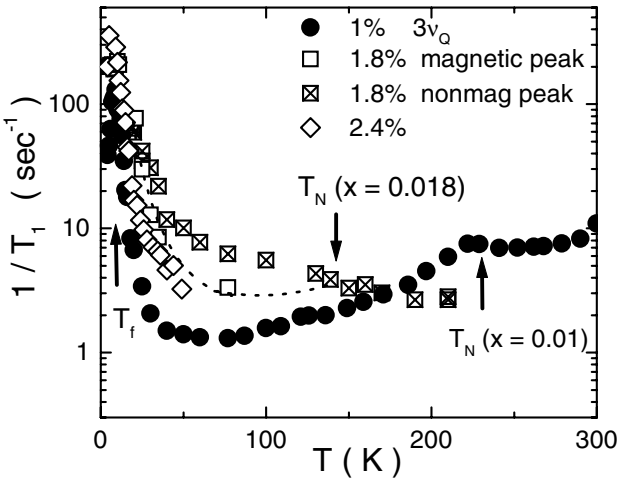

FIG. 4. T dependence of $1/T_1$ of La. $1/T_1$ in $x = 0.01$ is measured at $3\nu_Q$ transition. $1/T_1$ in $x = 0.018$ below T_N is measured at both the nonmagnetic site (6.3 MHz) and the magnetic site (5.75 MHz). The dotted curve is an eye guide of $1/T_1$ of the 1.8% magnetic peak.

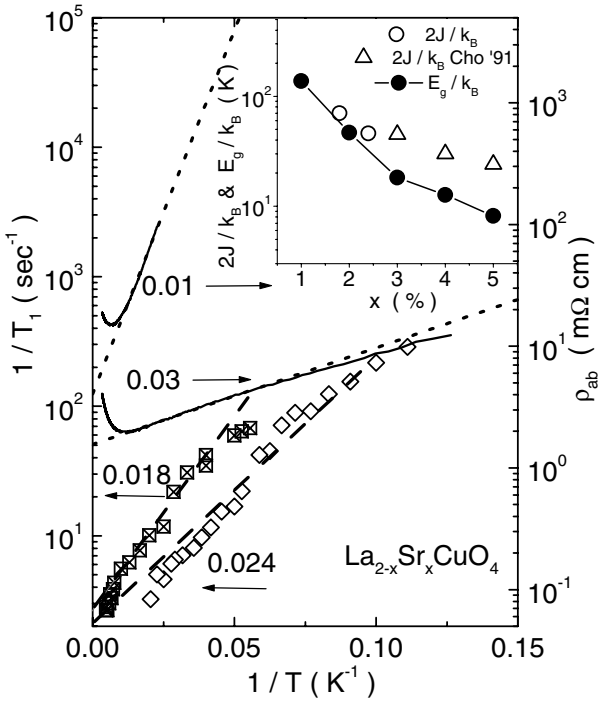

FIG. 5. $1/T_1$ at the nonmagnetic site in $x = 0.018$ and 0.024 is plotted against $1/T$ to estimate the characteristic energy of spin dynamics. In-plane resistivity in $x = 0.01$ and 0.03 is also plotted against $1/T$ to evaluate the charge excitation gap, E_g [9]. The inset shows the concentration dependence of present $2J/k_B$, $2J/k_B$ reported by Cho *et al.* [3] and E_g/k_B [9].

that the $1/T_1$ at the AFM and nonmagnetic sites for $x = 0.018$ follows the relation of $1/T_1 \sim \exp[2J(x)/k_BT]$ [2,3,12,13]. Therefore, τ_c shows a continuous increase as $\tau_0 \exp(2J/k_BT)$ with decreasing T. Here J is a characteristic energy of spin dynamics. In Fig. 5, the $1/T_1$ at the nonmagnetic site is plotted against $1/T$ to estimate the characteristic energy of $2J(x)$, together with the $1/T_1$ at $x = 0.024$. Thus estimated $2J$ is plotted against x in the inset of Fig. 5, where $2J/k_B$ reported by Cho *et al.* and E_g in charge transport are also plotted for comparison [3,9]. From ρ_{ab} increasing logarithmically upon cooling below 100 K, E_g is estimated from the relation of $\rho_{ab} \sim \exp(E_g/k_BT)$ as shown in Fig. 5 [9]. It is remarkable that $2J/k_B$ and E_g/k_B are quite similar in magnitude and dependence of x. $2J/k_B$ and E_g/k_B are related with a characteristic energy scale for spin excitations from the nonmagnetic or extended spin-singlet to a magnetic state and a gap in charge transport of mobile holes, respectively. These results strongly suggest that the spin dynamics at the nonmagnetic phase would arise from the charge transport caused by mobile holes. Taking these results into account, we remark the following conclusions: (i) in the slightly hole-doped Mott insulators at $x = 0.018$, Cu^{2+} derived spin fluctuations are enhanced by the charge dynamics of doped holes, reducing the AFM ordering T. The *metallic* behavior of mobile holes continues on passing through T_N. (ii) Therefore, the phase separation occurs due to the *partial destruction of AFM order* caused by mobile holes. (iii) As T decreases further, the mobility of holes becomes smaller, accompanying the gap E_g in charge transport. As a result, Cu-derived spin fluctuations are slowing down and the frequencies of fluctuations pass through ω_n around $T_f \sim 20$ K. Below T_f, spins are frozen, and the nonmagnetic phase is completely expelled due to the localization of holes. Taking into account that $H_{\rm int}^{ab}$ is unchanged upon the doping level, the size of moments is almost the same regardless of the doping level. We suggest that the cluster with homogeneous moments is aligned with the diagonal modulation below T_f affected by the localization of holes.

In conclusion, the La-NQR study has unraveled that the nonmagnetic phase persists to exist down to low T even though passing through the Néel temperature T_N, giving clear evidence for the novel magnetic phase separation for $x = 0.018$. As T decreases further well below T_N, it is a remarkable finding that the characteristic energy scale for spin excitations is comparable to the gap of charge transport of mobile holes. Furthermore, below $T_f \sim 20$ K, the localization of holes make spins freeze and then the size of spins are almost the same as that in the undoped La_2CuO_4. This novel phase separation is suggested as being due to the *partial destruction of AFM phase* caused by mobile holes via the formation of extended spin-singlet state between Cu-derived spins and hole spins.

The authors thank H. Kohno, K. Miyake, and M. Matsuda for valuable discussions. This work was supported by the COE Research (10CE2004) in Grant-in-Aid for Scientific Research from the Ministry of Education, Culture, Sport, Science, and Technology of Japan (MEXT), by the Grants-in-Aid for Scientific Research from Japan Society for Promotion of Science (JSPS), and by MEXT.

*Present address: Department of Physics, Kyoto University, Kyoto 606-8502, Japan.
†Present address: ASRC, Japan Atomic Energy Research Institute, Tokai, 319-1195, Japan.
‡Present address: Department of Physics, Okayama University, Okayama, 700-8530, Japan.
§Present address: IMR, Tohoku University, Sendai, 980-8577, Japan.

[1] B. Batlogg *et al.*, *Electronic Properties of High-Tc Superconductors* (Springer, Berlin, 1993), p. 5.
[2] F. C. Chou *et al.*, Phys. Rev. Lett. **71**, 2323 (1993).
[3] J. H. Cho *et al.*, Phys. Rev. B **46**, 3179 (1992).
[4] F. Borsa *et al.*, Phys. Rev. B **52**, 7334 (1995).
[5] M. Matsuda *et al.*, Phys. Rev. B **61**, 4326 (2000).
[6] S. Wakimoto *et al.*, Phys. Rev. B **60**, R769 (1999).
[7] M. Fujita *et al.*, Phys. Rev. B **65**, 064505 (2002).
[8] M. Matsuda *et al.*, Phys. Rev. B **65**, 134515 (2002).
[9] Y. Ando *et al.*, Phys. Rev. Lett. **87**, 017001 (2001).
[10] T. Suzuki *et al.*, Phys. Rev. B **66**, 172410 (2002).
[11] Ch. Niedermayer *et al.*, Phys. Rev. Lett. **80**, 3843 (1998).
[12] M.-H. Julien *et al.*, Phys. Rev. Lett. **83**, 604 (2002).
[13] N.J. Curro *et al.*, Phys. Rev. Lett. **85**, 642 (2000).